The spinning rotor gauge

J. K. Fremerey
Institut für Grenzflächenforschung und Vakuumphysik der Kernforschungsanlage Jülich GmbH, D 5170 Jülich, Federal Republic of Germany

(Received 19 September 1984; accepted 29 October 1984)

The determination of pressure in a high vacuum from the gaseous drag of a freely rotating sphere was already proposed in 1946 by Beams and co-workers. On the basis of novel techniques, this method was developed from its original bulky and delicate experimental state to a practicable, compact instrument for widespread laboratory and industrial use. The present paper gives a detailed description of the gauge head functions, and of the method of evaluation of the rotor deceleration rate. The predictability of the gaseous drag is discussed in view of absolute pressure gauging. The feasibility of extending the measurement range up to atmospheric pressure is demonstrated on the basis of experimental results.

I. INTRODUCTION

The investigation of rarefied gases by observation of the gaseous drag of rotating devices was introduced independently by Meyer[1] and Maxwell[2] about 120 years ago. The rotors were suspended by wires or fibers, hence their rotational motion was confined to a limited angle of deflection from the equilibrium position. The drag was calculated from the decrement of the maximum angular deflection of the freely oscillating device. A continuously rotating device appears advantageous over an oscillating one, as the drag can be evaluated from observation of times. This, however, was not applicable for a long time due to the nonreproducible drag associated with mechanical friction. The introduction of a magnetic rotor suspension by Holmes[3] therefore brought about great progress in the field and made feasible the actual spinning rotor gauge (SRG) which is free from mechanical friction and associated drag. In 1946, Beams and coworkers[4] first described the application of a magnetically suspended, freely rotating steel ball for determination of pressure in a high vacuum. The later development of a more practicable permanent magnetic rotor suspension[5–7] represents the main technical basis for the widespread use of the SRG. Commercial units nowadays provide a resolving power of 10^{-7} mb under routine working conditions. The historical development has been reviewed in a recent paper.[8]

We will give here a short review of the gauge head functions followed by a more detailed look at the method of processing the rotor speed signal. The development of the latter technique provides a second basis for the realization of an instrument for practical use. Noncorrelated measurement outputs are now available every few seconds, while conventional methods of signal processing at comparable resolving power require much longer measurement cycles. A central concern of the present paper will be the question whether, or to what extent, the SRG may be regarded as an absolute gauge. Some implicit assumptions associated with the SRG and with well-established primary vacuum standards will be discussed.

The feasibility of a wide-range SRG providing a linearized pressure scale from below 10^{-7} mb up to and above one atmosphere will be demonstrated at the end of this paper.

II. GAUGE HEAD FUNCTIONS

The basic functions of the SRG head are described with reference to Fig. 1. The rotor *R*, typically a 4.5 mm diam steel bearing ball, is magnetically suspended without mechanical contact on the axis of a nonmagnetic stainless steel tube *V*. The tube is connected to the vacuum system, typically via a CF 35 flange.

The rotor suspension is achieved by magnetic forces between two mutually attracting permanent magnets *M*. The axial positions of the magnets are properly adjusted so that when the rotor stays on the axis of tube *V*, the magnetic and gravitational forces on the rotor cancel. The equilibrium is unstable, i.e., the rotor will flip towards either the upper or lower magnet unless stabilization means are provided. These means consist of two electomagnet coils *A* which support the attraction of the lower magnet when the rotor moves upward and, vice versa, support the attraction of the upper magnet when the rotor moves downward. As a result, the rotor is steadily bound to the central equilibrium position. The coils are energized from a dc amplifier which is controlled by a dc

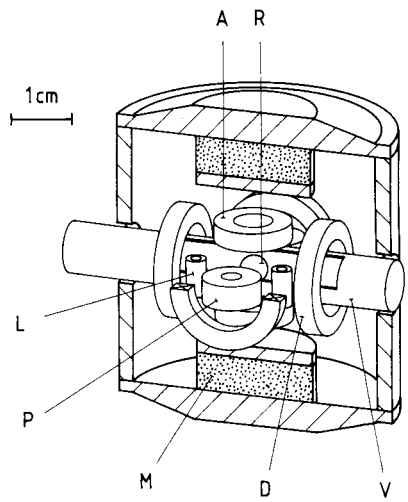

FIG. 1. SRG head: R—rotor; V—vacuum enclosure (partially cut away); M—one of two permanent magnets; A—one of two coils for pickup and control of axial rotor position; L—one of four coils of lateral damping system; D—one of four drive coils; P—one of two pickup coils.

 0734-2101/85/031715-06$01.00

sensing voltage. The latter is proportional to the vertical deviation of the rotor from the equilibrium position. The amplifier provides restoring and damping forces.

The dc sensing signal is best derived from the axial control coils A by means of a differential sensing circuit[7] which compares the rf impedances of these coils. The impedances slightly depend on the proximity of the rotor which picks up a tiny amount of rf power from the coils. When the rotor stays halfway between the coils, the sensing circuit output voltage and the control current become zero. Otherwise, the magnitude and polarity of these signals correspond to the rotor deviation along the vertical.

Within the lateral plane, the rotor favors the vertical axis of the magnets where the field is strong. In order to damp out lateral oscillations of the rotor which may occur and persist upon mechanical shock and/or vibration, four coils L are provided, two on each side of tube V. When the rotor moves towards or away from one of these coils then, due to the strong vertical magnetic polarization of the rotor, an inductive voltage appears at that coil. This voltage is proportional to the lateral velocity of the rotor. The amplified signal is connected to a corresponding control coil of similar shape which is placed right on the opposite side of the rotor. The magnetic moment generated by the control coil interacts with the rotor magnetic moment in such a way that the lateral movement along the direction between the corresponding coils is damped out quite efficiently. The second pair of coils works similarly, so that the rotor gets stabilized along any lateral direction. The damping time constant is about 1 s.

Four additional coils D connected to the output of a two-phase ac generator provide a rotating magnetic field for spinning the rotor about the vertical axis. The drive mechanism is similar to that of an ordinary induction motor. The rotor achieves a rotational speed of 400 Hz within less than 1 min. The generator is then cutoff, and the rotor is allowed to coast.

The freely spinning rotor slows down by the action of gas molecules. This mechanism will be described in Sec. IV. A small residual eddy current drag which typically is equivalent to the gaseous drag in air at some 10^{-6} mb has to be accounted for in any precise low pressure work. The residual drag can be determined while the system is pumped down to its base pressure. It remains stable over long periods of time unless the rotor is removed from the suspension. The residual drag will not be treated here, as this has been done in previous publications.[9–11]

The slowing down of the rotor is measured in terms of $-\dot{\omega}/\omega$, the relative deceleration rate of the rotor angular frequency ω. The deceleration rate is determined from observation of the zero crossings of an inductive pickup signal generated by the rotating component of the rotor magnetization. Two pickup coils P are provided for this purpose.

The occurrence of a pickup voltage is ascribed to a small inclination of the rotor magnetization against the spin axis. As the vertical spin axis does not move under stationary conditions,[10] the magnetization describes a small cone around the vertical. Thereby, the upper and lower poles of the rotor are alternately inclined towards either of the coils P. The variation of flux at the coils associated with that periodic inclination causes inductive voltages to appear at the coils which are in antiphase with each other. The coils must be properly connected in order to double rather than cancel the pickup signal. In the proper connection, this two-coil system suppresses all even harmonics of the pickup signal, while the reverse connection suppresses all odd harmonics, including the base signal. A distinct advantage of this pickup-coil arrangement when connected in the proper sense is that it also suppresses flat stray fields along the vertical. Such fields may be introduced by external electromotive equipment, e.g., by a pump drive, even though the gauge head mild steel housing provides quite effective magnetic shielding. The vertical orientation of the pickup coil axes also minimizes the inductive coupling to the rotor drive field.

III. EVALUATION OF THE ROTOR DECELERATION RATE

Present and potential users of the SRG sometimes feel uneasy with the method of evaluation of the rotor deceleration rate $-\dot{\omega}/\omega$ from the rotor speed signal. We feel that this matter should be explained in detail before entering the more general discussion given in Sec. IV on the qualification of the SRG as an absolute gauge.

As a basic thought, we should recognize the fact that $-\dot{\omega}/\omega$ as a differential quantity cannot be determined within zero time. Thus, measurements of this quantity always represent an average taken over some finite time interval. For the determination of $-\dot{\omega}/\omega$, we can use a variety of equivalent expressions composed of time intervals which are derived from the signal period, e.g.,

$$\langle -\dot{\omega}/\omega \rangle_{\mathrm{av}} = \begin{cases} (\tau_j - \tau_i)/(\tau_j \cdot \tau_i), & \text{(1a)} \\ 4(\tau_j - \tau_i)/(\tau_j + \tau_i)^2, & \text{(1b)} \\ [2(\tau_j' - \tau_i')/(\tau_j' + \tau_i')]/\tau_\Delta\ . & \text{(1c)} \end{cases}$$

The time intervals τ_i, τ_j and τ_i', τ_j' always comprise a certain number of consecutive rotor revolution periods. They will be called multiperiods. In Eqs. (1a) and (1b), multiperiods τ_i and τ_j themselves have to follow each other without a time delay,[9] while in the case of Eq. (1c), τ_i' and τ_j' need not necessarily be connected. Time intervals τ_Δ account for the separation between multiperiods τ_i' and τ_j'.

The method of evaluation of the deceleration rate from a primary pulse chain is explained with reference to Fig. 2. The central time axis symbolizes a uniform rotation, with time marks (short bars) occurring exactly at the times when the rotor crosses a given angular position. As the rotor slows down, the spacing of these time marks should increase a little towards the right. Thin vertical lines indicate the times when the pickup voltage crosses zero, thus marking the electrical trigger pulses. Two consecutive trigger marks define an elementary period τ_0 which itself is a multiple of the rotor revolution period. The elementary periods are identified by numbers as indicated close to the time axis. The random deviations δt of the trigger pulses around the rotor time marks correspond to the time jitter of the electric signal which is mainly due to thermal noise originating from the pickup coils.

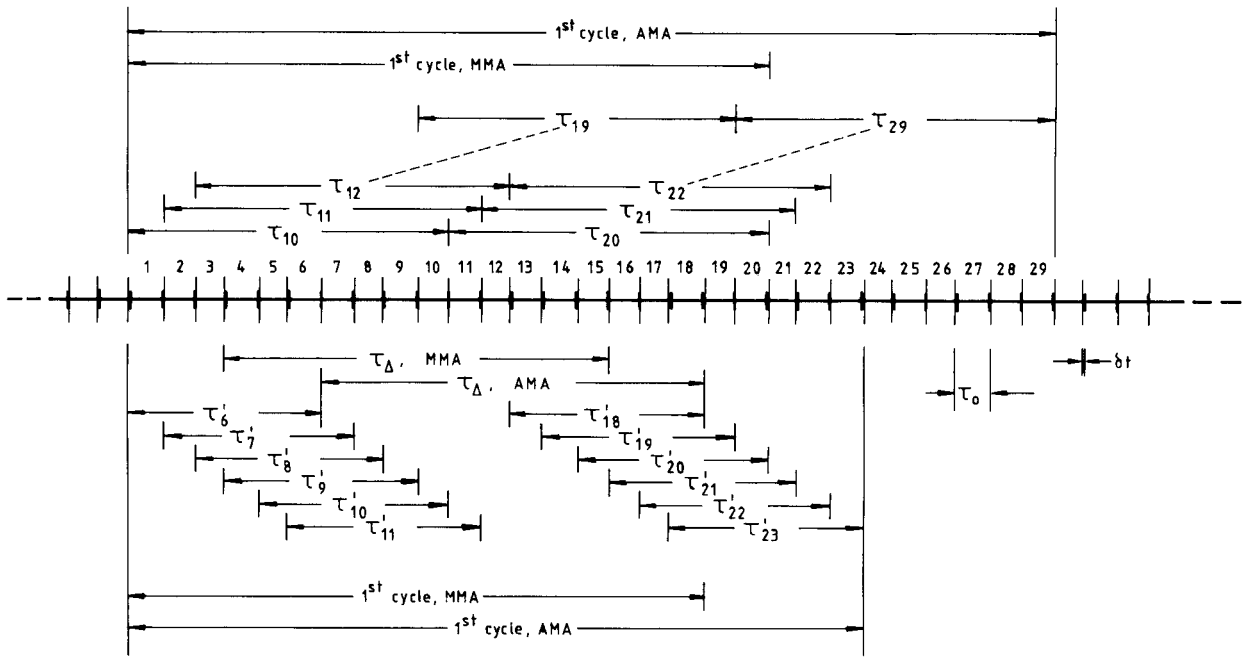

FIG. 2. Multiperiod configurations for calculation of SRG output scatter from signal scatter δt.

Typical distributions of multiperiods as employed in the SRG are indicated by dimension lines in Fig. 2. Subscripts indicate the number of the last elementary period contained in the respective multiperiod. Conventional multiperiod averaging is accomplished on the basis of Eqs. (1) by using two multiperiods which immediately succeed one another,[9] e.g., $\tau_i = \tau_{10}$ and $\tau_j = \tau_{20}$, or by using spaced multiperiod, e.g., $\tau'_i = \tau'_6$ and $\tau'_j = \tau'_{18}$.

The output rate of earlier SRG units at 10^{-7} mb resolution was only about two readings per minute.[5] A new technique now provides several multiperiod evaluations to be carried out in parallel, each one being separated in time from the next by one elementary period.[12] This method will be identified by MMA for multiple-track multiperiod averaging. When the multiperiods are composed of 10 elementary periods, as outlined in the example given in the upper section of Fig. 2, the first reading appears at the end of the 20th elementary period and all further outputs follow at distances of only one elementary period. In this way, the SRG output rate is augmented by a factor of 10. It should be pointed out, however, that the instrument response time does not reduce accordingly, i.e., independent readings will occur at distances of 20 elementary periods only, as before.

The MMA technique further provides a special averaging mode allowing for a considerable reduction of the output scatter.[12,13] In this mode, a certain number of consecutive multiperiods are summed up and the sums enter into Eq. (1). This averaging mode will be identified by AMA for accumulated multiperiod averaging. For the multiperiod distributions shown in Fig. 2, summing is carried out over multiperiods τ_{10} through τ_{19} and τ_{20} through τ_{29}, or τ'_6 through τ'_{11} and τ'_{18} through τ'_{23}. The first AMA outputs are available at the ends of τ_{29} and τ'_{23}, respectively, and the next ones appear at intervals of one elementary period. The instrument response time is increased by this averaging mode, i.e., independent outputs occur at distances of 29 and 24 elementary periods, respectively. The output scatter is reduced by the root of the number of consecutive multiperiods averaged over, i.e., by $\sqrt{10}$ and $\sqrt{6}$, respectively.

The mean deviation of the deceleration rates associated with the relative distributions of multiperiods as outlined in Fig. 2 is easily specified, on the basis of error calculus, in terms of δt and τ_0, and of τ, which represents the whole measurement cycle:

$$\text{MMA}\begin{cases}\delta_c(-\dot{\omega}/\omega) = & 4\sqrt{6}\delta t/\tau^2, \quad (2a)\\ \delta_s(-\dot{\omega}/\omega) = & 9\delta t/\tau^2, \quad (2b)\end{cases}$$

$$\text{AMA}\begin{cases}\delta_c(-\dot{\omega}/\omega) < & 27\sqrt{2\tau_0/\tau}\,\delta t/\tau^2, \quad (2c)\\ \delta_s(-\dot{\omega}/\omega) < & 32\sqrt{\tau_0/\tau}\,\delta t/\tau^2. \quad (2d)\end{cases}$$

Subscripts c and s indicate whether the multiperiods are connected or spaced, according to the upper and lower sections of Fig. 2, respectively. Figure 3 gives a graphical representation of Eq. (2a), and of Eq. (2d), with $\tau_0 = 2.5$ ms. A time

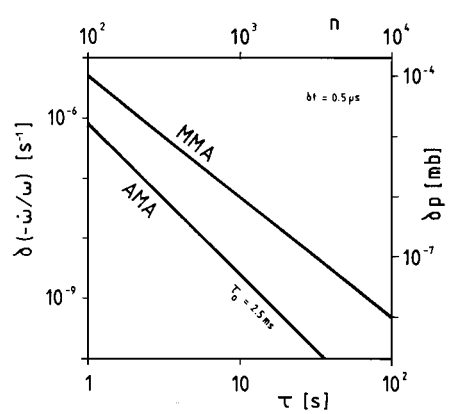

FIG. 3. Dependence of SRG output scatter on the length of measurement cycle τ according to Eqs. (2a) and (2d). Pressure variations δp correspond to 4.5 mm diam steel ball in argon and n denotes the number of multiperiods averaged over in the AMA mode, when $\tau_0 = 2.5$ ms.

jitter $\delta t = 0.5\ \mu s$ was assumed in both cases. These data are typical of the former and new versions of commercial SRG units.

We see that the reproducibility attainable within a given measurement time interval τ can be considerably improved by application of the AMA procedure, as compared to the MMA method. Alternatively, similar reliability can be achieved within much shorter measurement cycles by the AMA technique.[13]

A possible objection to the AMA technique has sometimes been aroused concerning the different weighting of the elementary periods in the accumulated multiperiods. From the viewpoint of statistical evaluation, however, it is essential that weighting of the random trigger deviations δt be uniform. In this sense, the relative distribution of multiperiods as shown in the lower section of Fig. 2 may be looked at as an optimum solution,[14] as each of the δt deviations takes part in the statistical evaluation, but does so only once.

IV. THE GASEOUS DRAG AND ITS PREDICTABILITY

There has been a lot of experimental evidence gathered in the past for the fact that gas molecules leaving a smooth adsorbate-covered metal surface on the average do not exchange any significant amount of tangential momentum with the surface, irrespective of their angle of incidence. Let us accept for the moment this experimental finding as a fact of general validity which, in particular, applies in the case of the SRG rotor. The absence of tangential momentum associated with the outgoing molecules implies that these molecules need not be considered in the calculation of the gaseous drag of a spherical rotor.

The tangential momentum transferred by the incident molecules is calculated by assuming that these molecules come from the walls of the vacuum enclosure without having collided with other molecules. In this case, the average tangential momentum transferred to the rotor amounts to $mr^2\omega$ per molecule, where m denotes the molecule mass, r the radial distance of the locus of impingement from the spin axis, and ω the rotor angular velocity. We further take into account the rate of impingement $(2/\pi)p/m\bar{c}$ which is expressed here in terms of the gas pressure p and mean molecular velocity $\bar{c}$. The integral action of the incident molecules causes a loss rate of angular momentum $-(8\pi/15)da^5\dot{\omega}$ of the spinning ball as expressed in terms of the ball radius a and material density d. Upon integration over the spherical surface, we easily obtain the gaseous drag in terms of the relative rotor deceleration in unit time

$$-\dot{\omega}/\omega = (10/\pi)(1/ad)p/\bar{c}. \tag{3}$$

This relationship has in fact been verified within a few per cent by numerous investigations on freely spinning rotors over the past 40 years.[4,15–25] Thus, the assumption made of the vanishing contribution of the outgoing molecules proves to be correct within the limits of experimental accuracy.

The early results of Hogg[26] (1906) and Knudsen[27] (1934), which were obtained from oscillating devices, are also well compatible with the above assumption. Nowadays, it can be shown by molecular beam experiments that the angular distribution of gas molecules rebounding from smooth adsorbate-covered metal surfaces is diffuse and almost perfectly symmetric with respect to the surface normal, even for glancing beam incidence.[28,29] A nice demonstration of the fact that the tangential momentum transfer does not depend, within experimental error, on the angle of incidence is given in a recent paper describing a novel detector for the determination of absolute molecular beam intensities.[30]

To the same extent that the above assumption holds, the SRG must be regarded as an absolute gauge. The requirement for an absolute gauge is that it need no calibation. The quantity to be determined must be reducible to fundamental quantities such as length, mass, and time, and other well-defined quantities which require no calibration. When looking at Eq. (3), we see that this condition applies for the SRG. The deceleration rate $-\dot{\omega}/\omega$, the radius a, and the density d of the rotor material are accessible by fundamental methods, and $\bar{c}$, the mean molecular velocity, is a quantity which can be predicted for any gas in equilibrium at a known temperature without calibration.

The qualification of a gauge as an absolute one does not tell anything about its accuracy. The accuracy rather depends on the reproducibility of the experimental conditions under which the measurements are carried out. As an example, let us have a look at a well-established fundamental high-vacuum standard, the static expansion apparatus.[31–33] The basic assumption associated with this apparatus is the applicability of Boyle's law, which says that for a given quantity of an ideal gas at a given temperature, the pressure is inversely proportional to the volume in which the gas is enclosed. Although the volume of the different expansion vessels contained in the apparatus can be determined by fundamental methods to within about 10^{-4} and the inlet pressures can be determined to similar precision, it is quite difficult to attain an accuracy of better than 1% by this method. One problem is to meet the condition that the quantity of gas remain constant during the expansion process. This depends on the gas–surface conditions at the inner walls of the expansion vessels and valves. It is well known that great care must be taken with these conditions in order to keep trapping and desorption of gases in a static expansion device at a low level. Therefore, static expansion standards are preferably used for calibration with noble and other inert gases. Calibration with reactive gases may severely affect accuracy due to nonpredictable adsorption and desorption processes, in particular at low calibration pressures.[32]

We can thus state that the qualification of an absolute standard in the case of the static expansion apparatus is based on the assumption of the applicability of Boyle's law and accuracy depends on the degree of its experimental verification. Similarly, we can state for the SRG that the qualification of an absolute gauge is based on the assumption that outgoing molecules on an average do not contribute to the rotor drag and accuracy depends on the degree of experimental verification of this condition.

We certainly feel much more comfortable with Boyle's law, which has been established by experience over the centuries, than we do with our experience concerning the outgoing molecules. We further know that Boyle's law can be de-

rived from fundamental theory and a theory on outgoing molecules is still missing. On the other hand, it appears that the experimental verification in the case of the SRG involves fewer restrictions than in the case of the static expansion apparatus. In particular, the SRG accuracy is principally not affected by reactive gases. On the contrary, these gases are expected to meet the requirements concerning the outgoing molecules almost perfectly, as they undergo complete accommodation to the surface by adsorption.

The main causes affecting the accuracy of an SRG may be traced back to: (i) coverage of the rotor surface with nonmetallic material; (ii) absence of adsorbates; and (iii) roughening of the rotor surface. The effect of these conditions is usually accounted for by a coefficient σ_{eff} on the right-hand side of Eq. (3). This coefficient denotes the apparent degree of accommodation of tangential momentum on the rotor surface. Under ideal conditions, on a perfect sphere we expect $\sigma_{\text{eff}} = 1$. Whenever we find $\sigma_{\text{eff}} < 1$, this necessarily indicates that a fraction of the incident tangential momentum is passed on to the outgoing molecules by specular reflection. Our basic assumption does not apply in this case. Reduced accommodation may occur under one of the above conditions (i) or (ii). The former may occur due to contamination with oil or grease and usually can be eliminated by chemical cleaning and bakeout. The error margin due to that sort of contamination in general does not exceed a few per cent. Condition (ii) has been achieved so far only by rigorous heat treatment at temperatures well above 1000 K,[34] or by deposition of clean metal films on clean substrates,[35] both procedures carried out in ultrahigh vacuum. However, the reduction of σ_{eff} below unity due to condition (ii) is quite unlikely to have any significant effect on SRG measurements under practical conditions, including bakeout at 700 K.

Condition (iii) can be provided, e.g., by chemical etching, or sand blasting. Experimental σ_{eff} values up to about 1.22 have been found on rough rotors.[17,20] Theoretical considerations suggest that a maximum value of 1.27 can be expected for an isotropically rough rotor.[8,36] Our basic assumption of a smooth surface does not apply in this case. Deviations of σ_{eff} above unity are explained by the geometrical structure of the rotor surface. A large fraction of the surface elements on a rotating rough ball does not move tangentially. Therefore, we have to use a different concept for calculation of the rotor drag than we did for calculation of Eq. (1).

Roughening of a rotor surface may cause trouble in certain SRG applications. For instance, if a polished steel ball is operated in a reactive gas, chemical etching of the steel surface may occur with σ_{eff} increasing by several per cent. For special applications, therefore, it is recommended to passivate the rotor surface by, e.g., a platinum coating.

An alternative method of stabilizing the σ_{eff} coefficient is to provide the rotor with a rough surface beforehand. This method has proved well in some recent work carried on at PTB, Berlin.[37] Obviously, the drag of a rough ball is essentially determined by momentum exchange on surface elements which are inclined with respect to the average tangential rotor surface. On an etched ball, the surface roughness is so steep that the rotor drag is predominantly determined by normal momentum exchange. The drag can then be predicted to a good approximation on the basis of mathematical expressions derived for the drag of a rotating vane.[36] The similarity of etched balls and vanes was demonstrated by experimental investigations.[20] The rotating vane gauge[38] is already known as an absolute gauge.[31] We conclude that an etched ball may also claim the qualification of an absolute pressure sensor.

V. EXTENSION TO HIGHER PRESSURES

The SRG operating range usually ends up at some 10^{-2} mb where the deceleration vs pressure characteristic (3) becomes increasingly nonlinear. The deviation from Eq. (3) towards higher pressures results from the nonisotropy of incident molecules which have been whirled up by collisions with molecules coming from the rotor. Concepts have been

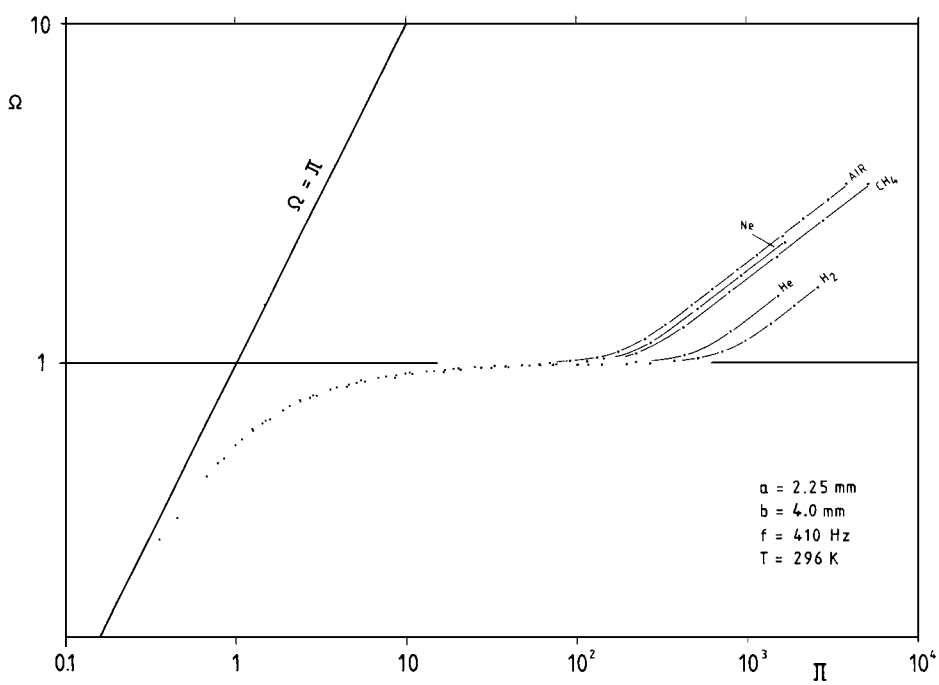

FIG. 4. Normalized deceleration vs pressure plot of SRG outputs obtained with different gases in a static pressure divider. High pressure branches end up at about one atmosphere.

devised for a linearization of SRG output data up to about 1 mb.[13,23] These concepts are based on the existence of a saturation level $(-\dot{\omega}/\omega)_{sat}$ of the deceleration rate at higher pressures. This level is essentially determined by the gas viscosity η and by the geometry of the interspace between the rotor and the vacuum enclosure.[39] Corrections were given in terms of a relative pressure p_i/p_{sat}, where p_i is the indicated pressure as calculated via Eq. (3) from the measured deceleration rate, and p_{sat} is calculated from Eq. (3) by inserting the viscous drag $(-\dot{\omega}/\omega)_{sat}$.

A modified concept now provides the introduction of a two-dimensional normalized plot of the deceleration vs pressure characteristics, as shown in Fig. 4, with $\Omega = (-\dot{\omega}/\omega)/(-\dot{\omega}/\omega)_{sat}$, and $\Pi = p/p_{sat}$, where $-\dot{\omega}/\omega$ is the measured deceleration rate and p is the real pressure.

At lower pressures, the experimental points obtained for a variety of gases follow a common curve within the normalized diagram. The very small increase of Ω over Π within the saturation regime in fact allows for useful pressure indications, provided that the variations of η with temperature can be compensated for. Otherwise, such variations, due to the heat fluctuations associated with the rotor drive, would simulate pressure variations by up to one order of magnitude. One can practically escape the problem by a new technique, which accounts for the temperature fluctuations. By this means, the resulting error of pressure indication within the saturation regime can be reduced to about 20%. Details will be reported in a separate paper.

Above some critical transient pressure Π_{tr}, Ω increases from the saturation level turning over into a straight line. This "high-pressure" characteristic persists up to and above atmospheric pressure and indicates the presence of boundary layer flow conditions at the rotor surface.[40] Experimentally, we find $\Pi_{tr} p_{sat} = C_{tr}\eta/M$, where M denotes the molecular weight of the gas and C_{tr} is a system constant which essentially depends on the rotor geometry and rotational speed. The general shape of the Ω vs Π characteristics within the total range from high vacuum up to atmospheric pressure can be described by the following relationship:

$$\Omega = f_{sat}(\Pi)\left[1 + (\Pi/\Pi_{tr})^{\alpha}\right]^{\beta}. \quad (4)$$

The high-vacuum and viscous-flow regimes are covered by a saturation function $f_{sat}(\Pi)$ which for low pressures reduces to $\Omega = \Pi$. Although analytical approximations can be given for f_{sat}, we found it more practicable to use a table representation for this function which is directly derived from the experimental plot. The boundary-layer regime is accounted for by the binomial term in Eq. (4). From the slope of the high-pressure branches in Fig. 4, we find $\alpha\beta \cong 0.39$, while the transition between the saturation and high-pressure branches fits well by splitting into $\alpha \cong 3$ and $\beta \cong 0.13$.

For evaluation of the real pressure $p = \Pi p_{sat}$ from the measured deceleration rate $-\dot{\omega}/\omega = \Omega(-\dot{\omega}/\omega)_{sat}$, the inverse function of Eq. (4) is required. Also for this purpose, Eq. (4) should preferably be represented by a table which can be read out in the reverse direction.

It will be a challenging task for the coming years to realize a wide-range SRG concept as outlined above at the level of a commercial series production.

ACKNOWLEDGMENTS

The author is very grateful to Professor George Comsa for having initiated and continuously supported the SRG development program at KFA-Jülich and for stimulating discussions. The contribution of valuable material by Messrs. Bernd Lindenau, Dr. Albrecht Weller, and Klaus Witthauer is also gratefully acknowledged.

[1] O. E. Meyer, Pogg. Ann. **125**, 177 (1865).
[2] J. C. Maxwell, Phil. Trans. R. Soc. **157**, 249 (1866).
[3] F. T. Holmes, Rev. Sci. Instrum. **8**, 444 (1937).
[4] J. W. Beams, J. L. Young, and J. W. Moore, J. Appl. Phys. **17**, 886 (1946).
[5] J. K. Fremerey, J. Vac. Sci. Technol. **9**, 108 (1972).
[6] J. K. Fremerey, Rev. Sci. Instrum. **44**, 1396 (1973).
[7] J. K. Fremerey and K. Boden, J. Phys. E **11**, 106 (1978).
[8] J. K. Fremerey, Vacuum **32**, 685 (1982).
[9] J. K. Fremerey, Rev. Sci. Instrum. **42**, 753 (1971).
[10] J. K. Fremerey, Rev. Sci. Instrum. **43**, 1413 (1972).
[11] J. K. Fremerey, Phys. Rev. Lett. **30**, 753 (1973).
[12] J. K. Fremerey, German Patent Appl. No. 29 14 072 (1979).
[13] J. K. Fremerey, B. Lindenau, and K. Witthauer, in Proceedings of the 9th International Vacuum Congress, Extended Abstracts Volume, Madrid (1983), p. 100.
[14] A. Weller (private communication).
[15] J. W. Beams, D. M. Spitzer, and J. P. Wade, Rev. Sci. Instrum. **33**, 151 (1962).
[16] P. J. Harbour and R. G. Lord, J. Sci. Instrum. **42**, 105 (1965).
[17] G. Comsa, J. K. Fremerey, and B. Lindenau, in Proceedings of the 7th International Vacuum Congress, Vienna (1977), Vol. I, p. 157.
[18] G. Comsa, J. K. Fremerey, B. Lindenau, G. Messer, and P. Röhl, J. Vac. Sci. Technol. **17**, 642 (1980).
[19] G. Messer, in Proceedings of the 8th International Vacuum Congress, Cannes (1980), Vol. II, p. 191.
[20] G. Comsa, J. K. Fremerey, and B. Lindenau, in Proceedings of the 8th International Vacuum Congress, Cannes (1980), Vol. II, p. 218.
[21] G. Messer and L. Rubet, in Proceedings of the 8th International Vacuum Congress, Cannes (1980), Vol. II, p. 259.
[22] Cong Shu-ren, Wan Yon-liang, and Lu Jia-huo, Vac. Sci. Technol. (China) **2**, 64 (1982).
[23] G. Reich, J. Vac. Sci. Technol. **20**, 1148 (1982).
[24] K. E. McCulloh, J. Vac. Sci. Technol. A **1**, 168 (1983).
[25] P. J. Van Ekeren, M. H. G. Jacobs, J. C. A. Offringa, and C. G. De Kruif, J. Chem. Thermodynamics **15**, 409 (1983).
[26] J. L. Hogg, Proc. Am. Acad. Arts Sci. **42**, 115 (1906).
[27] M. Knudsen, *The Kinetic Theory of Gases* (Methuen, London, 1934), p. 29.
[28] F. C. Hurlbut, J. Appl. Phys. **28**, 844 (1957).
[29] D. Auerbach, C. Becker, J. Cowin and L. Wharton, in *Proceedings of the 2nd International Symposium on Molecular Beams* (Noordwijkerhout, Netherlands, 1977), p. 192.
[30] K. Kern, B. Lindenau, R. David, and G. Comsa, Rev. Sci. Instrum. **56**, 52 (1985).
[31] K. F. Poulter, J. Phys. E **10**, 112 (1977).
[32] G. Messer, in Proceedings of the 7th International Vacuum Congress, Vienna (1977), Vol. I, p. 153.
[33] A. Berman, Vacuum **29**, 417 (1979).
[34] R. G. Lord, *Rarefied Gas Dynamics* (AIAA, New York, 1977), p. 531.
[35] L. B. Thomas and R. G. Lord, *Rarefied Gas Dynamics* (Academic, New York, 1974), p. 405.
[36] J. K. Fremerey, Proc. 4th ICSS and 3rd ECOSS, Cannes (1980), Vol. II, p. 869.
[37] G. Messer, P. Röhl, A. Calcatelli, D. A. Elkington, P. J. Nash, and L. Rubet, in Proceedings of the 9th International Vacuum Congress, Extended Abstracts Volume, Madrid (1983), p. 83.
[38] R. Evrard and G. A. Boutry, J. Vac. Sci. Technol. **6**, 2 (1969).
[39] D. M. Greig and T. H. Wise, *Hydrodynamics and Vector Field Theory* (The English Universities, London, 1962), p. 202.
[40] F. P. Bowden and R. G. Lord, Proc. R. Soc. London Ser. A **271**, 143 (1963).